

# Dynamic Smagorinsky model on anisotropic grids

A. Scotti and C. Meneveau

Department of Mechanical Engineering, Johns Hopkins University, Baltimore, Maryland 21218

M. Fatica

Center for Turbulence Research, Stanford, California 94305-3030

(Received 3 December 1996; accepted 11 February 1997)

To examine the performance of the dynamic Smagorinsky model in a controlled fashion on anisotropic grids, simulations of forced isotropic turbulence are performed using highly anisotropic discretizations. The resulting model coefficients are compared with an earlier prediction. Two extreme cases are considered: pancake-like grids, for which two directions are poorly resolved compared to the third, and pencil-like grids, where one direction is poorly resolved when compared to the other two. © 1997 American Institute of Physics. [S1070-6631(97)01406-2]

The aim of this Brief Communication is to study the performance of the dynamic Smagorinsky model on complicated grid geometries. Consider, as an example, Large eddy simulation (LES) of the flow past a 3-D bluff body: near the object, one needs to refine the grid in the spanwise directions. For a structured mesh, far downstream the grid may be greatly expanded in the streamwise direction. Therefore, the grid can be strongly anisotropic, with elements looking like sheets or pencils, depending on the kind of refinement imposed upstream. Hence, in the far-wake region one may have a situation where the computational grid is highly anisotropic, even if the turbulence is not far from isotropic.

In LES, the grid filter is dictated by the computational mesh used to solve the equations (although, for methods other than spectral, it is difficult to give a precise definition of the filtering operator associated with a given discretization). Classical eddy-viscosity models need as input a length-scale which is usually associated to the scale at which the filter operates. It is problematic to define this length when, as a result of the anisotropy of the grid, the filter is defined by more than one length scale. For the Smagorinsky model, this problem was considered first by Deardoff<sup>1</sup> and later by Schumann,<sup>2</sup> Lilly<sup>3</sup> and Scotti *et al.*,<sup>4</sup> although in the last two papers only theoretically.

On the other hand, the dynamic model does not in principle require a length scale to be specified. The question then arises whether this model is able to correctly simulate isotropic turbulence on anisotropic grids. The main goal of this work is to examine this question.

The non-dynamic Smagorinsky model for the SGS stress is written as

$$\tau_{ij} = -2[\mathcal{L}(\Delta_1, \Delta_2, \Delta_3)]^2 |\tilde{S}| \tilde{S}_{ij}, \quad (1)$$

where  $|\tilde{S}| = \sqrt{2\tilde{S}_{lm}\tilde{S}_{lm}}$  is the strain-rate magnitude. Here  $\Delta_1, \Delta_2$  and  $\Delta_3$  are the dimensions of the computational cell which will be assumed to pertain to the inertial range. For notational convenience and without lack of generality, let us assume  $\Delta_1 \leq \Delta_2 \leq \Delta_3$ . Introducing  $\Delta_{eq} = (\Delta_1 \Delta_2 \Delta_3)^{1/3}$ ,  $\mathcal{L}(\Delta_1, \Delta_2, \Delta_3)$  can be written as

$$\mathcal{L}(\Delta_1, \Delta_2, \Delta_3) = C_s \Delta_{eq} f(a_1, a_2), \quad (2)$$

where  $a_1 = \Delta_1/\Delta_3$  and  $a_2 = \Delta_2/\Delta_3$  are the two aspect ratios of the grid.  $C_s$  is the traditional Smagorinsky constant appropriate for isotropic grids. For the original Deardoff<sup>1</sup> approach,  $f = 1.0$ . In Ref. 4 it was shown, based on theoretical arguments for isotropic turbulence, that an improved estimate is

$$f(a_1, a_2) \approx \cosh \sqrt{\frac{4}{27}[(\log a_1)^2 - \log a_1 \log a_2 + (\log a_2)^2]}. \quad (3)$$

In the dynamic version of this model,<sup>5,4</sup> with grid filtering denoted by tilde and test filtering by an overbar, the length-scale  $\mathcal{L}(\tilde{\Delta}_1, \tilde{\Delta}_2, \tilde{\Delta}_3)$  is computed according to

$$[\mathcal{L}(\tilde{\Delta}_1, \tilde{\Delta}_2, \tilde{\Delta}_3)]^2 = \frac{\langle L_{ij} M_{ij} \rangle}{\langle M_{ij} M_{ij} \rangle}, \quad (4)$$

where  $\langle \cdot \rangle$  denotes volume averaging,  $L_{ij} = \overline{\tilde{u}_j \tilde{u}_i} - \tilde{u}_i \tilde{u}_j$  and using Eq. (2)

$$M_{ij} = 2 \left[ \overline{|\tilde{S}| \tilde{S}_{ij}} - \left( \frac{\overline{\Delta_{eq}}}{\tilde{\Delta}_{eq}} \frac{f(\bar{a}_1, \bar{a}_2)}{f(\tilde{a}_1, \tilde{a}_2)} \right)^2 |\tilde{S}| \tilde{S}_{ij} \right]. \quad (5)$$

If test and grid filters have the same aspect ratios, then Eq. (4) is closed and no expression for  $f(a_1, a_2)$  is required. Otherwise one can use Eq. (3) to compute  $f$  and check *a posteriori* its consistency.

In order to compare the various approaches we perform LES of isotropic turbulence in a periodic box of side  $2\pi$ . Turbulence is maintained by a forcing  $\mathbf{f}$  on the largest modes ( $k \leq 2$ ) with an intensity such that the energy injection rate  $\mathbf{f} \cdot \mathbf{u}$  is fixed to a constant value  $\varepsilon = 1.0$ . The molecular viscosity is set to zero. The numerical scheme is the same as in Vincent and Meneguzzi.<sup>6</sup> It uses Adam–Bashforth 2 for time stepping, with  $\Delta t = 0.001$ . The non-linear terms, written in rotational form, are evaluated pseudo spectrally. The grids have aspect ratios  $a_1 = \Delta_1/\Delta_3$ ,  $a_2 = \Delta_2/\Delta_3$  ranging from 1 to 1/16. Grid filtering was performed with a sharp spectral cut-off setting to zero the modes outside the ellipsoid

$$B = \{\mathbf{k} \in R^3 | (k_1 \Delta_1)^2 + (k_2 \Delta_2)^2 + (k_3 \Delta_3)^2 \leq 8/9 \pi^2\},$$

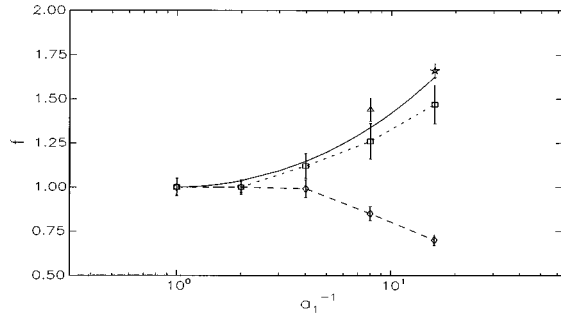


FIG. 1. Time averages of  $f_{\text{dyn}}(a_1, a_2)$  for pancake-like grids,  $a_2 = 1$  (boxes), and pencil-like grids  $a_2 = a_1$  (diamonds). The solid line is the theoretical prediction of Eq. (3). The triangle and the star are  $f_{\text{dyn}}$  for, respectively, a pencil-like and a pancake-like grid but using isotropic test filtering. Error bars are  $\pm \sigma$ , where  $\sigma$  is the standard deviation about the time average.

which has the advantage of partially removing aliasing errors. Sufficient additional alias control was achieved by random phase shifts (see Ref. 7), since selected runs using the  $\frac{2}{3}$ -rule showed no difference in results.

Computations are performed using the classical non-dynamic Smagorinsky model with the Deardoff length scale and  $f = 1$ , as well as with the Smagorinsky model corrected after Ref. 4 including  $f(a_1, a_2)$  as evaluated from Eq. (3). In both cases  $C_s^2 = 0.026$ . The dynamic model uses test filtering at a scale twice as large as the grid in all directions. In all cases the initial condition is assumed to be a Gaussian field with  $k^{-5/3}$  spectrum, random phases and total kinetic energy equal to unity.

To obtain a self-consistent estimate for the dynamic Smagorinsky constant we first run LES with the dynamic model with isotropic spherical test and grid filter, on a  $32^3$  grid. After an initial transient the value stabilizes at  $C_s^2 = 0.023 \pm 5\%$ . Next, we perform LES on anisotropic grids characterized by aspect ratios  $a_1$  and  $a_2$ . The dynamic results are cast in terms of  $f(a_1, a_2)$ , by writing

$$f_{\text{dyn}}(a_1, a_2) = \sqrt{\frac{\langle L_{ij} M_{ij} \rangle}{2C_s^2 \Delta_{eq}^2 \langle M_{ij} M_{ij} \rangle}},$$

where  $C_s^2 = 0.023$ .

Figure 1 shows the result for different values of the aspect ratios, compared to the predictions of Eq. (3). The dynamic model reproduces the correct trend for pancake-like grids, but fails with pencil-like grids. To examine the simulations more closely, we now focus on two extreme cases: a  $256 \times 16 \times 16$  grid (pancake) and a  $128 \times 128 \times 16$  grid (pencil). For each case, we compare the dynamic model with predictions of the non-dynamic Smagorinsky model and with the non-dynamic model but including the correction of Eq. (3).

Properties such as total kinetic energy, derivative skewness in the least resolved direction, etc., are well reproduced by all models for both pancake and pencil cases. In the following we concentrate on the small scale behavior, as quantified by 1-D pre-multiplied spectra.

For isotropic turbulence we know that the spectral tensor in the resolved inertial range should be given by

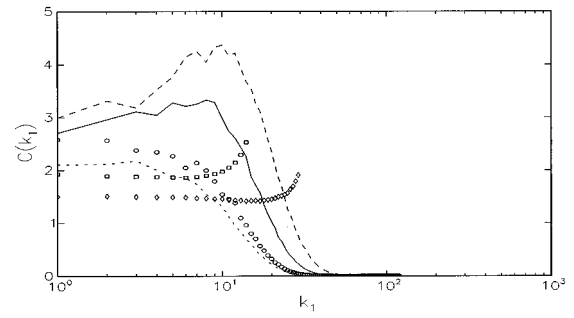


FIG. 2. Pre-multiplied 1-D spectrum of eddy-viscosity models on a pancake-like grid: Smagorinsky–Deardoff (dashed line), modified Smagorinsky (dotted line), dynamic model (solid line), and dynamic model with isotropic test filter (circles). The squares show  $C(k_1)$  computed from a simulation using the dynamic model on an  $32^3$  isotropic grid, diamonds are for a  $64^3$  grid.

$$Q_{ij}(\mathbf{k}) = \langle \tilde{u}_i(\mathbf{k}) \tilde{u}_j(-\mathbf{k}) \rangle = (4\pi)^{-1} C_K \varepsilon^{2/3} k^{-11/3} P_{ij}(\mathbf{k}),$$

where  $\varepsilon$  is the average dissipation,  $C_K$  is the Kolmogorov constant and  $P_{ij}(\mathbf{k})$  is the projector on the space orthogonal to  $\mathbf{k}$ . Instead of simply multiplying the spectrum by  $k^{5/3}$ , due to the anisotropy of the grid, it is better to study the “filter-weighted” 1-D pre-multiplied spectra, defined as

$$C(k_1) = \frac{\int_B 2\pi \varepsilon^{-2/3} k^{11/3} Q_{ii}(\mathbf{k}) dk_2 dk_3}{\int_B dk_2 dk_3}. \quad (6)$$

For ideal Kolmogorov turbulence,  $C(k_1)$  is a constant equal to the Kolmogorov constant  $C_K \approx 1.6$ .

For pancake-like grids the results are shown in Fig. 2. The traditional Smagorinsky–Deardoff case shows a strong peak (pile up) at wave number  $k_1 \sim 10$ . The modified Smagorinsky case remains constant at small wave numbers, and dies out at high wave numbers, without showing any pile-up. The dynamic model results fall somewhere in between, but slightly higher than the expected value of  $C_K$ . All models show a rapid decay at wave numbers above 10. The fact that all three models decay for  $k_1 > 10$  means that those modes that cannot have access to all the local triadic interactions experience a high drain of energy so that they do not display a Kolmogorov scaling. It appears unlikely that any modification of a scalar eddy-viscosity model could compensate for this behavior.

In the case of pencil-like grids (Fig. 3), as in all cases, scales between the least and best resolved directions are much less energetic than the Kolmogorov spectrum, as is clear from the rapid drop of the pre-multiplied spectrum above  $k_1 = 16$ . For the dynamic model,  $C(k_1)$  is much too large, about twice as high as expected. Therefore, the “underestimation” of  $f$  observed in Fig. 1 brings consequences that cannot be ignored at the scales near the least resolved direction (due to the integration over  $k_2$  and  $k_3$  in Eq. (6), even at low  $k_1$  there is an effect of pile-up at high  $k_2$  and  $k_3$ ).

The derivative skewness in the best resolved direction is consistent with these differences: we find that the smaller the skewness in magnitude, the more the energy piles up.

In order to understand the causes of this behavior, we recall that the dynamic model computes  $\mathcal{L}$  by sampling the turbulence between grid and test filter. It could be argued

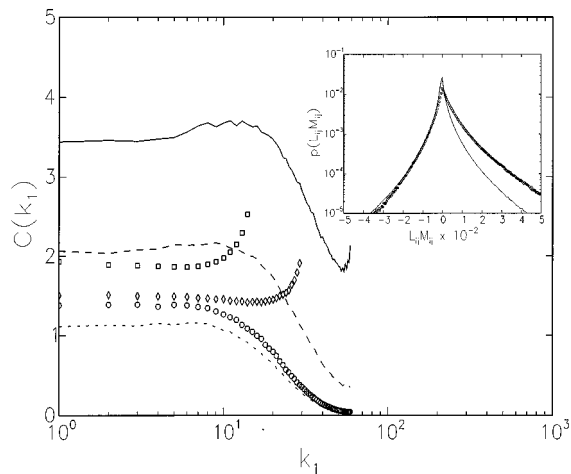


FIG. 3. Premultiplied 1-D spectrum of eddy-viscosity models on a pencil-like grid (see Fig. 2 for symbols explanation). The inset shows the PDF of  $L_{ij}M_{ij}$  with same grid but different test filters of the dynamic model for pencil-like grid: anisotropic test-filter (solid line), isotropic test filter (circles).

that for pencil-like grids these modes behave essentially as 2-D turbulence, with the vorticity aligned in the least resolved direction ( $x_3$ ) and a concomitant change in the dynamic. To focus on the relevant scales, we analyze the vorticity band-pass filtered between test and grid filter (i.e., the statistics of  $\omega' = \hat{\omega} - \bar{\omega}$ ). We find that the variances are not isotropic, and that  $\omega_1'^2/\omega_3'^2 \sim \omega_2'^2/\omega_3'^2 \sim 0.75$ , i.e., the flow is not quite 3-D but not 2-D either. More directly related to the small value of  $\mathcal{L}$  or  $f_{\text{dyn}}$  obtained from the dynamic model, in Fig. 3 (inset) we show the PDF of  $L_{ij}M_{ij}$  (solid line). The curve is almost symmetrically distributed around the origin, and the average value, while positive, is very small ( $\langle L_{ij}M_{ij} \rangle = 4.80$ ).  $L_{ij}M_{ij}$  can be regarded as a measure of energy transfer from large to small scales, with negative values meaning energy backscatter. If we now compute the same PDF but using an isotropic test filter at a scale  $2\Delta_3$  in all three directions, we see that the shape of the PDF changes, being now skewed to the right (symbols in the inset of Fig. 3). The mean value is now  $\langle L_{ij}M_{ij} \rangle = 31.66$ . Therefore, by sampling larger scales that are more isotropic, the dynamics of the energy transfer changes noticeably.

This observation suggests that in order to improve the performance of the dynamic model in such extreme cases of grid anisotropy, it may be advisable to use a test filter which is isotropic, with a length scale twice as large as the worst resolved scale. In this case, the grid and test anisotropies

differ, and this must be taken into account explicitly in the dynamic model formulation. We now implement the dynamic model with Eq. (5) for  $M_{ij}$ , using the expression given in Eq. (3) for  $f(\bar{a}_1, \bar{a}_2)$  and  $f(\tilde{a}_1, \tilde{a}_2)$ . Using this formulation on a  $256 \times 16 \times 16$  simulation yields the result shown in Fig. 2, while the result for a  $128 \times 128 \times 16$  grid is shown in Fig. 3.

The resulting  $f_{\text{dyn}}$ 's oscillate around an average value of  $1.66 \pm 0.08$  and  $1.44 \pm 0.134$  respectively (see symbols in Fig. 1). At large scales the difference between these runs and the previous ones are very small. On the other end, at small scales the situation changes as now the premultiplied spectrum for pencil-like grid lies flat at 1.4 for  $k_1 < 10$ , much closer to the expected value of  $C_K$ . For the pancake-like grid, the premultiplied spectrum also falls closer to a constant  $C_K$ , although it is still somewhat larger.

It is concluded that isotropic test filtering improves predictions of the dynamic model when dealing with highly anisotropic grids. Perhaps not surprisingly, this conclusion is similar to one reached by others in the context of dynamic LES using non-spectral numerical methods, such as low-order finite differences. There, it has been found advisable to ‘‘prefilter’’ the results and shift the test filter to larger scales<sup>8</sup> so that the dynamic model is not strongly affected by numerical errors occurring near the grid scale.

## ACKNOWLEDGMENTS

We thank J. Jimenez, P. Moin, W. Cabot, D. Carati, and T. Lund for interesting discussions on this subject. This work was initiated at the CTR during the 1996 Summer School. The support of CTR and of NSF (CTS-9408344) is gratefully acknowledged.

- <sup>1</sup>J. W. Deardoff, ‘‘A numerical study of three-dimensional turbulent channel flow at large Reynolds numbers,’’ *J. Fluid Mech.* **41**, 453 (1970).
- <sup>2</sup>U. Schumann, ‘‘Subgrid scale model for finite difference simulations of turbulent flows in plane channels and annuli,’’ *J. Comput. Phys.* **18**, 386 (1975).
- <sup>3</sup>D. K. Lilly, ‘‘The length scale for sub-grid-scale parametrization with anisotropic resolution,’’ *Annual Research Briefs, Center for Turbulence Research* (1988).
- <sup>4</sup>A. Scotti, C. Meneveau, and D. K. Lilly, ‘‘Generalized Smagorinsky model for anisotropic grids,’’ *Phys. Fluid A* **5**, 2306 (1993).
- <sup>5</sup>M. Germano, U. Piomelli, P. Moin, and W. H. Cabot, ‘‘A dynamic subgrid-scale eddy viscosity model,’’ *Phys. Fluid A* **48**, 273 (1991).
- <sup>6</sup>A. Vincent and M. Meneguzzi, ‘‘The spatial structure and statistical properties of homogeneous turbulence,’’ *J. Fluid Mech.* **225**, 1 (1991).
- <sup>7</sup>A. Scotti, C. Meneveau, and M. Fatica, ‘‘Dynamic Smagorinsky model on anisotropic grids,’’ *Proceedings of the CTR Summer Program, 1996*.
- <sup>8</sup>T. S. Lund and H.-J. Kaltenbach, ‘‘Experiments with explicit filtering for LES using a finite-difference method,’’ *Annual Research Briefs, Center for Turbulence Research* (1995).